Available online at www.sciencedirect.com

ScienceDirect

Procedia Manufacturing 26 (2018) 372–382

Procedia MANUFACTURING

www.elsevier.com/locate/procedia

46th SME North American Manufacturing Research Conference, NAMRC 46, Texas, USA

Effect of Directional Relations on Milling Chatter Stability and Development of a Stability Index

Mukhtar Maulimov[a] and Burak Sencer[a]*

[a]*Oregon State University, Corvallis, 97331, USA*

* Corresponding author. Tel.: +1-541-737-5919; fax: +0-000-000-0000 .
E-mail address: burak.sencer@oregonstate.edu

Abstract

This paper analyzes effect of directional relationships on chatter vibrations experienced in peripheral milling process. Based on the directional relationships, a geometry-based chatter stability index (CSI) is proposed to improve chatter stability of the process. It is well-known that chatter stability depends on cutting conditions and tool geometry; whereas it is less known that it also depends strongly on the directional relations between the machining process and the flexible directions of the machine. In this research, these directional factors affecting chatter stability are extracted from process kinematics and dynamically compliant directions of the structure. Three cases are considered and analyzed; namely, 1) if the machine tool/workpiece structure is flexible only in single direction, 2) if it is flexible in two orthogonal directions and finally 3) when those flexible directions are not orthogonal. Tool feed direction is considered to be the optimization parameter to maximize process stability. Overall, this research aims to present new knowledge on the effect of directional relationships for chatter stability and how they can be utilized in a practical manner based on a chatter stability index (CSI) that can be computed from geometry, process kinematics and limited knowledge of machine dynamics.

Peer-review under responsibility of the scientific committee of the 46th SME North American Manufacturing Research Conference.

Keywords: regenerative chatter vibration; chatter stability index; asymptotic stability limit; milling;

1. Introduction

Chatter vibrations have been a major problem in various machining operations such as in turning, milling, boring and grinding [1]. It causes shorter tool life, poor surface quality and low productivity. Many researchers have investigated analysis of the self-excited chatter vibrations and clarified the mechanisms at various conditions for various operations [2]. It is well known that chatter stability depends on cutting conditions and tool geometry such as width or depth of cut and the spindle speed. Some

2351-9789
Peer-review under responsibility of the scientific committee of the 46th SME North American Manufacturing Research Conference.
10.1016/j.promfg.2018.07.045

researchers applied this knowledge to generate chatter-free tool paths [3]. On the other hand, it is less known that chatter stability also depends on tool path/posture relative to the dynamically most compliant direction [4]. Authors previously clarified importance of this tool path/posture for chatter stability and proposed a simple chatter stability index(CSI) for turning process to realize a quick and practical tool path/posture optimization [5]. This research extends that past work and proposes a chatter stability index for relative stability of peripheral milling processes.

In milling, several directions play significant role in process stability. Firstly, the feed direction between tool and workpiece plays a key role [6]. It controls the average force direction [5] jointly with the radial immersion [2] of the tool. For instance, if force direction is aligned perpendicular to the flexible direction of machine/workpiece structure, forced vibrations can be minimized attenuating regenerative effects and thus overall chatter stability could be improved. Thus, the flexible, i.e. compliant, directions of machine/workpiece structure are critical. Typically structures exhibit one or two dominant flexible directions that are orthogonal in conventional CNC machines. However, flexibilities on a robotic machining system can be non-orthogonal [6,7].

This paper tries to utilize geometry-based directional relationships to analyze chatter stability in milling. The objective is to generate an insight on how those directions can be used to optimize tool feed direction to maximize the chatter free material removal rate. Although, a simple chatter stability index (CSI) based on purely geometric relationships could be generated for case of milling with single dominant flexible direction, in case of 2D orthogonal and non-orthogonal flexible structures, the proposed formulations provide preliminary insight for optimizing feed direction to attain high chatter-free material removal. The paper is laid out as follows. First, effect of direction relations in milling for the case of structures with a single flexible direction is considered. A geometry-based asymptotic chatter stability index, CSI is then proposed to attenuate regenerative chatter vibrations. Next, two orthogonal flexible structure is considered and asymptotically chatter stability index including mode coupling is presented. Finally, in the case of non-orthogonal flexibility, the effect of feed direction on maximizing chatter stability is investigated. Simulation studies are used to validate accuracy of proposed techniques.

Note that, the proposed chatter stability index (CSI) in this paper is based on the asymptotic stability limit [2]. Asymptotic stability limit presents the borderline depth of cut which guarantees stable cutting regardless of spindle speed. In this work, it is used as a measure of relative stability.

2. Geometric chatter stability index in milling

The literature on chatter stability is extensive [8,9,10,11]. Typically, dynamic interaction of milling process with a flexible structure can be modeled by block diagram shown in Fig. 1 [12].

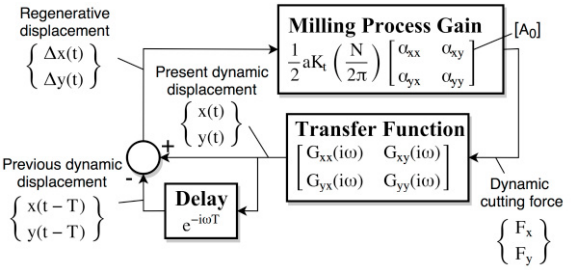

Fig. 1. Block diagram of milling process with regenerative chatter

The transfer function block contains directional frequency response functions. Milling process gain block dictates the relationship between chip thickness and cutting forces. Due to the kinematics of the process, chip thickness varies with spindle rotation so as the cutting forces. If directional cutting coefficients in milling process are averaged over one tooth period, chatter stability lobes would be very similar to the case when they are not averaged [2]. As a result, it is accustomed that chatter stability in time-varying milling process is analyzed by averaging cutting force variations [2].

2.1. Chatter stability for single degree of freedom systems

Fig. 2 depicts kinematics of peripheral milling. In this particular case, the machine/workpiece structure is assumed to have only a single dominant flexible (compliant) direction. This flexible direction can be determined either by experience, measurement, or through simulation. If the system has only a single flexible direction, it can only vibrate in that direction [13]. The well-known example is thin-walled workpiece machining [14,15]. Vibrations leave a wavy surface with fluctuating cutting area, which is called a regenerative effect.

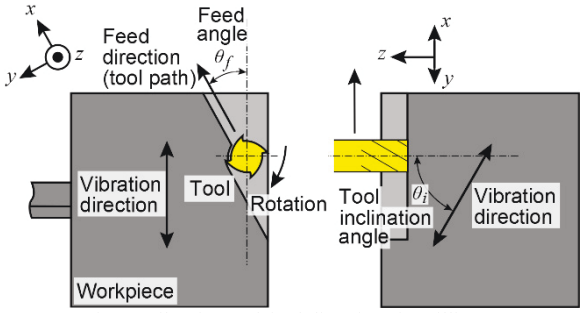

Fig. 2. Vibration and feed directions in milling process

Regenerative effect generates dynamic cutting forces with undesired phase lag causing cutting process to become unstable. The dynamic cutting area due to regenerative effect can be approximated by the product of the vibration amplitude projected onto the regenerative plane and the axial depth of cut. The regenerative plane (See Fig. 3) contains regeneration direction vector that is parallel to the radial cutting direction and the axial cutting direction vector. Thus, if the tool path/posture is rotated to align the regeneration plane perpendicular to vibration direction, regenerative effect can actually be eliminated. As a result, regenerative chatter vibrations could be avoided. As shown in Fig. 3, the angle α between vibration direction and the plane perpendicular to the regenerative plane can be used to evaluate a relative chatter stability index, which we call as the CSI here.

Let us define a unit displacement vector in the vibration direction (flexible direction) as $\vec{d} = \left[\sin\theta_i \cos\theta_f \quad \sin\theta_i \sin\theta_f \quad \cos\theta_i\right]^T$, shown in Fig. 2. Then, an instantaneous regeneration direction vector can be defined as a unit vector $\vec{n} = \left[\sin\phi \quad \cos\phi\right]^T$, where ϕ is the angle between cutting edge and y-axis as shown in Fig. 4.

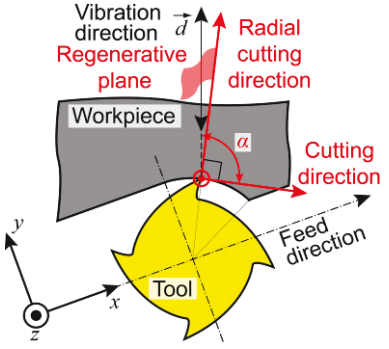

Fig. 3. Instantaneous tool edge regenerative direction

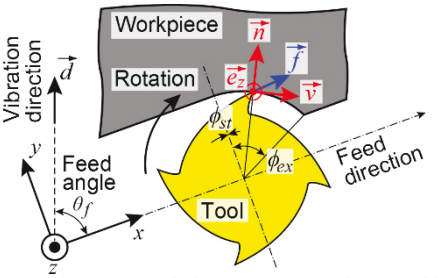

Fig. 4. Unit vectors to derive regenerative chatter stability index in milling process

The dynamic cutting area A can be expressed by the multiplication of axial depth of cut a and the inner product of regenerative direction vector with the unit vibration vector $A = a\vec{n}\cdot\vec{d} = a\sin\alpha$. If the regeneration direction vector is perpendicular to the displacement vector or vibration direction, i.e. $\alpha = 0$, the dynamic cutting area will not change, meaning that the regenerative effect can be suppressed.

The second directional factor affecting chatter stability is relation between vibration direction and the cutting force direction. As in the first directional factor case, if the direction of the resultant cutting force is perpendicular to the vibration direction, cutting forces cannot excite the structure. As a result, chatter vibrations will not grow. The angle β between vibration direction and a non-excitation plane, plane perpendicular to the resultant cutting force direction, can be used to evaluate the relative chatter stability index. The angle β is illustrated in Fig. 5.

For known cutting force coefficient ratios K_r and K_a [16], ratio of radial cutting force component and axial cutting force component to tangential cutting force component, respectively, a unit instantaneous

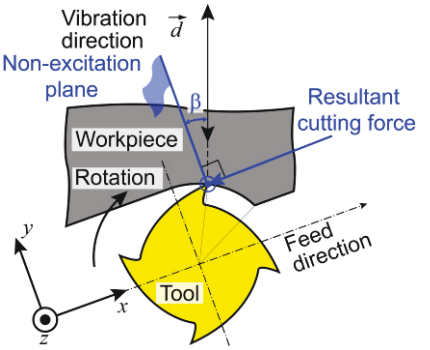

Fig. 5. Instantaneous resultant cutting force

cutting force vector can be defined as $\overrightarrow{f_u} = \left(\vec{v} + K_r \vec{n} + K_a \overrightarrow{e_z}\right) / \sqrt{1 + K_r^2 + K_a^2}$ and cutting forces will be $\overrightarrow{f} = A\overrightarrow{f_u}$. The instantaneous cutting force component in vibration direction becomes $f_e = \overrightarrow{f} \cdot \vec{d} = A\overrightarrow{f_u} \cdot \vec{d} = a \sin\alpha \sin\beta$. If the instantaneous cutting force direction is perpendicular to the vibration direction, i.e. $\beta = 0$, chatter vibrations will not grow.

Next, in milling operation, the average regenerative effect can be utilized. Average excitation force is found by integrating the instantaneous cutting force over one revolution, $\overline{f_e} = \overline{a \sin\alpha \sin\beta} = \left(N \int_{\varphi_{st}}^{\varphi_{ex}} f_e \, d\varphi\right) \Big/ 2\pi$, where N is the number of teeth. Finally, the regenerative chatter stability index for peripheral milling process can be written as:

$$I_{rcs} = \frac{1}{\left|\overline{f_e}\right|} = \frac{1}{\left|\overline{a \sin\alpha \sin\beta}\right|} \tag{1}$$

Note that, α and β can be computed based on known vibration direction $\vec{d}$. β is computed from the average cutting force direction as presented above, which can be obtained analytically by employing average milling force coefficient matrix $[A_0]$ [2]. Thus, Eq. (1) can also be written as:

$$I_{rcs} = \frac{1}{a\left|A_0 \vec{d}\right|} \tag{2}$$

2.2. Verification of regenerative stability index (CSI) for milling with single compliant direction

This section presents how the CSI index can be used to predict the relative stability limit and how feed/cutting direction can be used to maximize the stable material removal rate (MRR). Simulations conditions are summarized in Table 1. In this case the structure is assumed to be flexible only in a single direction along the vibration direction as depicted in Fig. 4. The feed and inclination angles, θ_f and θ_i (See Fig. 2), are varied. Analytical results based on the full chatter stability model [2] are shown in Fig. 6. The color map shows analytically predicted asymptotic critical axial depth of cut at each tool inclination and feed direction. As observed, when the tool feed and inclination directions are altered, asymptotic depth of cut could be increased greatly. Next, Fig. 7 presents CSI calculated from Eqs. (1) or (2) based on

Table 1. Simulation conditions for milling process

Cutting conditions	Axial depth of cut, a	1 mm for I_{rcs} calculations
	Radial immersion	0-π/3 rad (up milling)
	Number of teeth	2
Specific cutting force coefficients	Tangential	2000 MPa
	Radial	1200 MPa
	Axial	440 MPa
Structural flexibility (aligned with $\vec{d}$)	Mass	10 kg
	Static stiffness	10 N/μm
	Damping coefficient	300 N/(m/s)
	Vibration direction	Varied

geometrical relationships without using any transfer function data. As seen, the proposed simple CSI index accurately captures relative stability. Note that the white straight broken lines (A) indicate the directional relation where α=0, and the white curved broken line (B) corresponds to the other relation where β=0. Along those lines, regenerative chatter vibrations can be

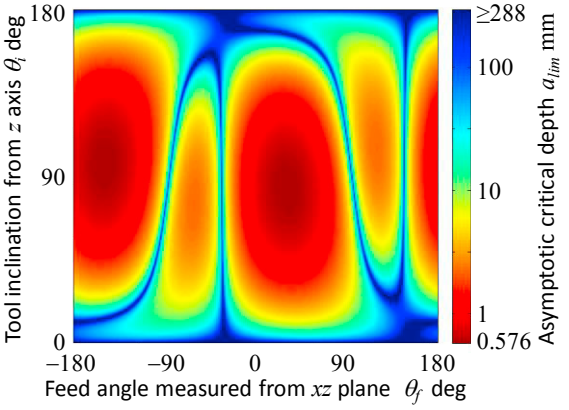

Fig. 6. Analytically predicted gain margin

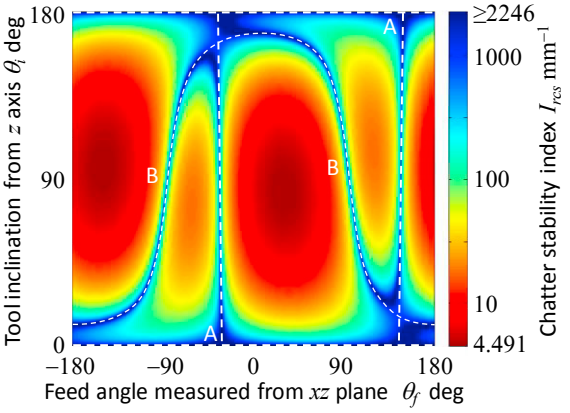

Fig. 7. Regenerative chatter stability index

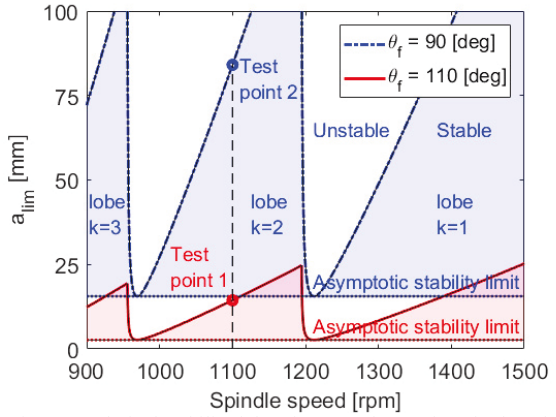

Fig. 8. Analytical stability lobes for 90 and 110 [deg] feed angles.

completely eliminated, and the process can achieve infinite stability enabling large depth of cuts. Thus, by simply altering tool feed and inclination directions the MRR can be maximized and proposed CSI can predict it accurately.

Please also note that Figs. 6 and 7 represent asymptotic stability limit, i.e. the relative stability. Compete stability lobes are also generated in Fig. 8 for the feed angles 90 [deg] and 110 [deg] whereas inclination angle is set to 120 [deg] and radial immersion is fixed to 60 [deg]. As observed from Figs. 6 and 7, the relative stability increases when feed angle is changed from 90 to 110[deg]. The increase in the asymptotic depth of cut is calculated as 483.82% from Fig. 8. Now, consider cutting at 1100 [rpm] under a lobe, when the asymptotic stability limit is increased by altering feed direction the maximum stable depth of cut is again increased by 483.82% even considering the lobe effect (See Fig.8). Thus, this concludes that once asymptotic stability limit is increased based on CSI, overall chatter free MRR is increased regardless of spindle speed. Note that, this case is strictly true when chatter vibrations originate from regenerative effect.

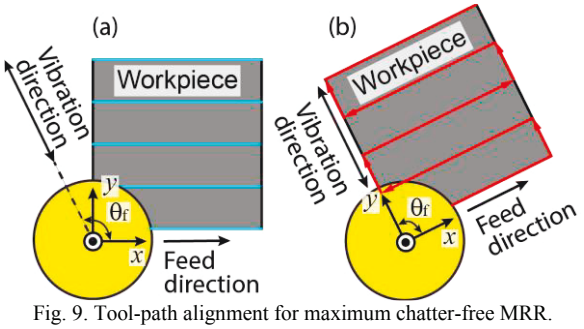

Fig. 9. Tool-path alignment for maximum chatter-free MRR.

Finally, Fig. 9 illustrates how feed direction can be utilized to maximize MRR. During basic face milling operations, the tool-path, i.e. the feed direction, is aligned such that regenerative vibrations are attenuated. This kind of path-planning strategy can be implemented easily in CAD/CAM systems since it is purely geometry based.

3. Definition of CSI for 2DOF systems

This section analyses directional effects on milling chatter stability in a more general case when mechanical structure contains flexibilities in two different directions [17]. As opposed to the approximation made in the previous section where the structure contains only a single dominant flexibility, most machine tools, or robotic machining systems [7,18,19,20] are flexible in two directions as shown in Fig. 10. These flexibilities can be attributed to the tool/tool-holder/spindle interface [21] or the machine and the workpiece [7].

The vibration direction is critical in finding abovementioned geometry-based relationships. However, in 2DOF systems, chatter vibration direction cannot be determined in a straightforward fashion. The following section first attempts to determine the vibration direction during chatter.

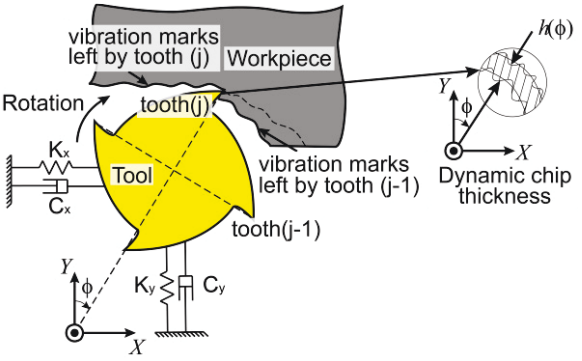

Fig. 10. Tool/workpiece structure with two orthogonal dynamics

3.1. Analysis of vibration trajectories for structures with two flexible directions

Firstly, the flexible system is considered to have degrees of freedom in X and Y directions, i.e. a set of orthogonal modes as shown in Fig. 8. Cutting forces excite the structure causing dynamic displacements in both X and Y directions. In this case, based on the regenerative chatter loop (Fig. 1), closed-loop milling dynamics may generate linear or elliptical vibrations

[22]. The vibration type and locus can be found from eigenvectors of the characteristic equation [23]. If eigenvectors are real, the system vibrates linearly in the direction of the eigenvectors. On the other hand, when the eigenvectors are complex, chatter vibration trajectory becomes elliptical. In that case, a major and a minor axis of the elliptical vibration locus can be determined.

Milling dynamics during chatter vibration can be analyzed by writing the closed loop dynamics from Fig. 1 and inspecting the eigenvalues from the characteristic equation [2]:

$$\det\left[\left[I\right]-\frac{1}{2}aK_t\left(1-e^{-i\omega_c T}\right)\left(\frac{N}{2\pi}\left[A_0\right]\right)\left[\Phi(i\omega_c)\right]\right]=0 \quad (3)$$

where K_t is the tangential cutting force component, a is the axial depth of cut, and $\left[\Phi(i\omega_c)\right]$ is the complex valued frequency response function with $\Phi_{xx}(i\omega)$, $\Phi_{xy}(i\omega)$, $\Phi_{yx}(i\omega)$ and $\Phi_{yy}(i\omega)$ being direct and cross transfer functions. Note that $\left[A_0\right]$ contains the directional cutting force coefficients,

$$\left.\begin{aligned}
\alpha_{xx}&=\frac{1}{2}\left[\cos(2\phi)-2K_r\phi+K_r\sin(2\phi)\right]_{\phi_{st}}^{\phi_{ex}}\\
\alpha_{xy}&=\frac{1}{2}\left[-\sin(2\phi)-2\phi+K_r\cos(2\phi)\right]_{\phi_{st}}^{\phi_{ex}}\\
\alpha_{yx}&=\frac{1}{2}\left[-\sin(2\phi)+2\phi+K_r\cos(2\phi)\right]_{\phi_{st}}^{\phi_{ex}}\\
\alpha_{yy}&=\frac{1}{2}\left[-\cos(2\phi)-2K_r\phi-K_r\sin(2\phi)\right]_{\phi_{st}}^{\phi_{ex}}
\end{aligned}\right\} \quad (4)$$

where ϕ_{st} and ϕ_{ex} are the entry and exit immersion angles as depicted in Fig. 11.

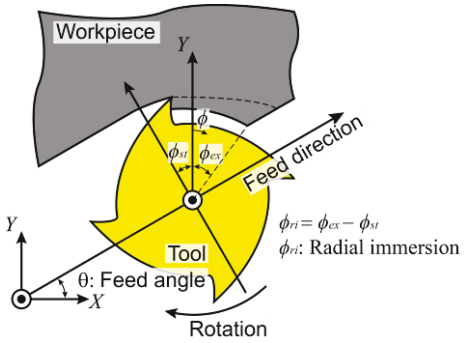

Fig. 11: Entry and exit angles of tool edge during cutting

Most machine tool structures are dominated by the tool mode, which allows use to assume, $\Phi_{xy}(i\omega)=\Phi_{yx}(i\omega)=0$ and $\Phi_{xx}(i\omega)=\Phi_{yy}(i\omega)$. These assumptions help simplify the characteristic equation from Eq. (3), to:

$$\det\left[\left[I\right]+\lambda\left[A_0\right]\right]=0 \quad (5)$$

where $\lambda=-\frac{N}{4\pi}aK_t\left(1-e^{-i\omega_c T}\right)\Phi_{xx}(i\omega_c)$. Solution of Eq. (5) reveals two cases. Eigenvalues are real if the determinant of the characteristic equation is real. Or, the eigenvalues become complex, which generates elliptical vibration trajectory and hence closed-form geometric relationships cannot be derived conveniently. Therefore, in this paper we first search the case in which chatter vibrations occur on a linear trajectory, i.e. eigenvalues are real.

Note that from Eq.5 that the directional coefficients $\left[A_0\right]$ control eigenvalues of the closed loop system. Expanding Eq. (5) yields following condition for strictly real eigenvalues, i.e. the discriminant of Eq. (5) is non-negative:

$$\left(\alpha_{xx}+\alpha_{yy}\right)^2-4\left(\alpha_{xx}\alpha_{yy}-\alpha_{xy}\alpha_{yx}\right)\geq 0 \quad (6)$$

Rewriting above inequality by plugging in directional coefficients from Eq. (4) reveals that the radial immersion ϕ_{ri} controls the vibration trajectory, i.e. the eigenvalues. By setting ϕ_{ri} as:

$$\left(\frac{\phi_{ri}}{\sin\phi_{ri}}\right)^2\leq K_r{}^2+1 \quad (7)$$

ensures that linear chatter vibrations are observed. Note that K_r is the ratio between the radial cutting coefficient and the tangential cutting coefficient, and ϕ_{ri} is the radial immersion, i.e. $\phi_{ri}=\phi_{ex}-\phi_{st}$. Therefore, limiting radial immersion to attain linear

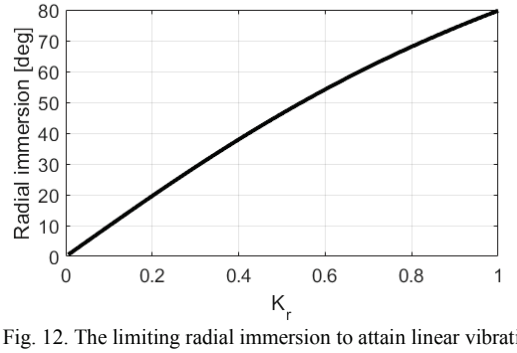

Fig. 12. The limiting radial immersion to attain linear vibration

vibrations can be plotted for variety of radial cutting force ratios as in Fig. 12. For various K_r values the immersion must be below the limiting curve.

The direction of vibration is then determined from normalized eigenvectors of the characteristic equation (Eq. (5)) as:

$$v_1 = \left[\frac{\lambda\alpha_{xy}}{\sqrt{\left(\lambda\alpha_{xy}\right)^2 + \left(1+\lambda\alpha_{xx}\right)^2}} \quad \frac{-\left(1+\lambda\alpha_{xx}\right)}{\sqrt{\left(\lambda\alpha_{xy}\right)^2 + \left(1+\lambda\alpha_{xx}\right)^2}} \right]^T$$
$$v_2 = \left[\frac{1+\lambda\alpha_{yy}}{\sqrt{\left(\lambda\alpha_{yx}\right)^2 + \left(1+\lambda\alpha_{yy}\right)^2}} \quad \frac{-\lambda\alpha_{yx}}{\sqrt{\left(\lambda\alpha_{yx}\right)^2 + \left(1+\lambda\alpha_{yy}\right)^2}} \right]^T \quad (8)$$

where v_1 and v_2 are identical, $v_1 = v_2$, for the same eigenvalue λ. They are identical because when Eq. (5) is solved for eigenvalue λ, the columns of $[I]_{2x2} + \lambda[A_0]_{2x2}$ matrix are linearly dependent. This will result in two linearly dependent eigenvector equations that will provide two identical eigenvectors for each of the eigenvalues of Eq. (5).

Overall, this section analyzed vibratory behavior of milling based on the characteristics equation. It is shown that radial immersion controls the vibration trajectory. By limiting radial immersion, linear chatter vibrations can be generated. Based on this analysis the following section tries to generate geometry based relative chatter stability index for the 2D case.

3.2. CSI for orthogonal 2DOF milling case

Section 2.1. showed that, when the system has a single flexible direction, mode coupling [22] is avoided, and regenerative chatter vibrations could be mitigated by setting vibration direction to be parallel to either to the average non-regeneration plane or the average non-excitation plane. This can be achieved by controlling the feed direction during cutting. However, when the structure has two flexible directions, as indicated by Eq. (8), vibration direction depends on the directional cutting coefficients. A relationship between regeneration direction and vibration direction, and between the average cutting force direction and vibration direction can be found as follows.

Firstly, the relation between average cutting force direction and vibration direction is analyzed. Assume that the vibration direction vector is a unit vector with components Δx and Δy in x and y directions. Then, the dynamic cutting forces can be written [2] as:

$$\begin{Bmatrix} F_x \\ F_y \end{Bmatrix} = \frac{N}{4\pi} a K_t \begin{bmatrix} \alpha_{xx} & \alpha_{xy} \\ \alpha_{yx} & \alpha_{yy} \end{bmatrix} \begin{Bmatrix} \Delta x \\ \Delta y \end{Bmatrix} \quad (9)$$

Since chatter vibration occurs in the direction of eigenvectors $v_1 = v_2$, their components are plugged into Δx and Δy in Eq. (9) to rewrite the cutting force as follows,

$$\begin{Bmatrix} F_x \\ F_y \end{Bmatrix} = \frac{N}{4\pi} a K_t \left(\frac{-1}{\lambda}\right) \begin{Bmatrix} \Delta x \\ \Delta y \end{Bmatrix} \quad (10)$$

Similar to Section 2.1, the angle β between vibration direction and average non-excitation plane, shown in Fig. 13, can be used to evaluate the relative chatter stability index. Note from Eq. (10) that λ is a real scalar. Thus, if it is positive valued, the average cutting force direction becomes aligned with the vibration direction but out of phase as shown in Fig. 13, which makes β=90.

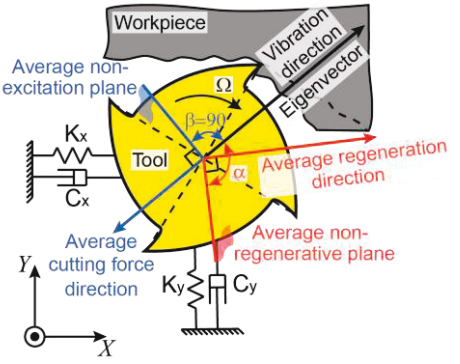

Fig. 13. Average cutting force, average regeneration and vibration directions in orthogonal 2DOF systems

Similarly, relationship between the average regeneration direction and vibration direction can be analyzed as follows. The average regeneration direction is found by integrating x and y components of dynamic chip thickness [2], $h(\phi) = \Delta x \sin(\phi) + \Delta y \cos(\phi)$, shown in Fig. 10, where ϕ is defined as the angle between cutting edge and y-axis. The instantaneous regeneration direction is $\vec{r} = \left[h(\phi)\sin\phi \quad h(\phi)\cos\phi\right]^T$. Then, the average regeneration direction is obtained by taking the integral of instantaneous regeneration direction over one revolution as follows:

$$\mathbf{R} = \frac{N}{2\pi}\int_{\phi_{st}}^{\phi_{ex}} \vec{r}\, d\phi \quad (11)$$

Here, $\mathbf{R}$ is the average regeneration direction with R_x and R_y components in x and y directions, respectively. Inserting the dynamic chip thickness into instantaneous regeneration direction, $\vec{r}$, and integrating above equation, Eq. (11) can be rewritten as,

$$\begin{Bmatrix} R_x \\ R_y \end{Bmatrix} = \frac{N}{2\pi} \begin{Bmatrix} \left[\frac{\Delta x}{2}\left(\phi - \frac{1}{2}\sin(2\phi)\right) - \frac{\Delta y}{4}\cos(2\phi) \right]_{\phi_{ex}}^{\phi_{st}} \\ \left[-\frac{\Delta x}{4}\cos(2\phi) + \frac{\Delta y}{2}\left(\phi - \frac{1}{2}\sin(2\phi)\right) \right]_{\phi_{ex}}^{\phi_{st}} \end{Bmatrix} \quad (12)$$

Using Eq. (9), the average cutting force direction can be expressed as:

$$\begin{Bmatrix} F_x \\ F_y \end{Bmatrix} = \frac{N}{4\pi} a K_t \begin{Bmatrix} \alpha_{xx}\Delta x + \alpha_{xy}\Delta y \\ \alpha_{yx}\Delta x + \alpha_{yy}\Delta y \end{Bmatrix} \quad (13)$$

and plugging in the cutting coefficients from Eq. (4), into Eq. (13) and rearranging Eq. (13) using Eq. (12), allows us to re-postulate the average cutting force direction in terms of the regeneration direction as:

$$\begin{Bmatrix} F_x \\ F_y \end{Bmatrix} = a K_t \begin{Bmatrix} -R_y - K_r R_x \\ -K_r R_y + R_x \end{Bmatrix} \quad (14)$$

Then, simultaneously solving equations (10) and (14), yields the expression for average regeneration direction:

$$\begin{Bmatrix} R_x \\ R_y \end{Bmatrix} = \frac{N}{4\pi\lambda(K_r^{\,2}+1)} \begin{Bmatrix} K_r\Delta x - \Delta y \\ \Delta x + K_r \Delta y \end{Bmatrix} \quad (15)$$

Next, the geometric relationship between average regeneration and the vibration directions can be defined based on Fig. 13 as:

$$\mathbf{R}\cdot\mathbf{\Delta x} = |\mathbf{R}||\mathbf{\Delta x}|\cos(\alpha - \pi/2) \quad (16)$$

where $\mathbf{R}$ is the average regeneration vector, i.e. $\mathbf{R} = \begin{bmatrix} R_x & R_y \end{bmatrix}^T$, $\mathbf{\Delta x}$ is the vibration direction, i.e. $\mathbf{\Delta x} = \begin{bmatrix} \Delta x & \Delta y \end{bmatrix}^T$, and the α is the angle between perpendicular direction to the average regeneration vector and vibration direction as shown in Fig. 13. Similar to Section 2.1, the angle α can also be used to evaluate the relative chatter stability index and α can be solved from Eq. (16) as:

$$\sin\alpha = \frac{K_r}{\sqrt{K_r^{\,2}+1}} \quad (17)$$

Above relation indicates that α, the directional relationship between the vibration and average regeneration directions is controlled by the ratio of cutting force coefficients, K_r. Thus, for constant radial immersions, changing cutting direction, or rotating DOF does not have any effect on the chatter stability.

Please note that cutting forces are calculated as multiplication of cutting force coefficient to dynamic cutting area. The dynamic cutting area is controlled by the regeneration effect, i.e. dynamic chip thickness. Average cutting force is average of instantaneous cutting forces over one revolution. It indicates that the average cutting force magnitude will include magnitude of the average regeneration vector. Therefore, in chatter stability index calculations, a unit average regeneration vector will be used so that only its directional effect can be taken into consideration in CSI. Let us define a unit average regeneration vector to be $\boldsymbol{R_u}$, normalized average regeneration vector or normalized version of Eq. (15). Thus, the final asymptotic chatter stability index is calculated by projecting the average cutting force vector and unit average regeneration vector onto the vibration direction. Then taking its reciprocal, the chatter stability index for 2D orthogonal case becomes,

$$CSI = \frac{1}{|\mathbf{F}||\mathbf{R_u}|\sin\alpha\sin\beta} \quad (18)$$

where $\mathbf{F} = \begin{bmatrix} F_x & F_y \end{bmatrix}^T$ is the average cutting force.

Please also note that above index is very similar to the one presented in previous chapter for the case when the structure has only single degree of freedom. However, in the 2DOF with orthogonal mode case, the term $\sin\alpha$ is only controlled by the cutting force ratio, K_r, which is constant. The angle β is constant and β=90 [deg]. From Eq. (10), the magnitude of the cutting force is $|\mathbf{F}| = (NK_t/4\pi)(a/\lambda)$. Thus, disregarding the constant terms from Eq. (18), the resultant relative asymptotic stability index can be simplified to:

$$CSI = \frac{\lambda}{a} \quad (19)$$

where λ is eigenvalue of characteristic equation, which can be computed from the roots of Eq. (5):

$$\lambda = \frac{-a_1 \pm \sqrt{a_1^{\,2} - 4a_0}}{2a_0} \quad (20)$$

where $a_1 = \alpha_{xx} + \alpha_{yy}$ and $a_0 = \alpha_{xx}\alpha_{yy} - \alpha_{xy}\alpha_{yx}$.

Plugging the directional cutting coefficients from Eq. (4), into Eq. (20), the eigenvalues become only the function of K_r and radial immersion;

$$\lambda = \frac{K_r\phi_{ri} \pm \sqrt{\left(K_r^{\,2}+1\right)\sin^2\phi_{ri} - \phi_{ri}^{\,2}}}{2\left(K_r^{\,2}+1\right)\left(\phi_{ri}^{\,2} - \sin^2\phi_{ri}\right)} \tag{21}$$

which concludes that CSI can only be computed from immersion and cutting force ratio.

3.3. CSI for non-orthogonal 2DOF case

In previous section, it was shown that when the system has two orthogonal modes, asymptotic chatter stability is only controlled by radial immersion and ratio between cutting force coefficients. This section considers the case when modes are not orthogonal. This case is more typical for 5-axis machine tools or in robotic machining [24].

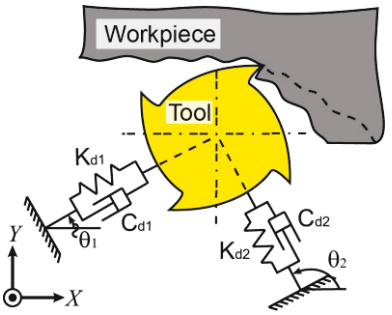

Fig. 14. Tool/workpiece structure with 2 non-orthogonal dynamics

The two flexible directions of the structure are defined by their orientation from the X axis θ_1 and θ_2 as show in Fig. 14 as $\vec{d_1} = [\cos\theta_1 \ \sin\theta_1]^T$ and $\vec{d_2} = [\cos\theta_2 \ \sin\theta_2]^T$. The characteristic equation for chatter stability is re-written from Eq. (3) for this case:

$$\det\left[[I] - \frac{1}{2}aK_t\left(1-e^{-i\omega_c T}\right)\left(\frac{N}{2\pi}\mathbf{Q}^T[A_0]\mathbf{Q}\right)[\Phi(i\omega_c)]\right] = 0 \tag{22}$$

where $\mathbf{Q} = \left[\vec{d_1} \quad \vec{d_2}\right]$ contains the flexible directions. Note from Eq. (22) that the non-orthogonal modes manipulate $[A_0]$ matrix:

$$A_0^{\,*} = \mathbf{Q}^T \ A_0 \ \mathbf{Q} \tag{23}$$

which in return imposes further directional relationship to the chatter stability. In other words, when the modes are not orthogonal, chatter stability can be controlled by changing the cutting, e.g. feed direction. This can be confirmed by solving the roots of Eq. (22). The eigenvalues from Eq. (22), are calculated as:

$$\lambda^* = \frac{-a_1 \pm \sqrt{a_1^{\,2} - 4a_0}}{2a_0} \tag{24}$$

where $a_1 = \alpha_{xx}^{\,*} + \alpha_{yy}^{\,*}$ and $a_0 = \alpha_{xx}^{\,*}\alpha_{yy}^{\,*} - \alpha_{xy}^{\,*}\alpha_{yx}^{\,*}$, and $\alpha_{xx}^{\,*}$, $\alpha_{xy}^{\,*}$, $\alpha_{yx}^{\,*}$ and $\alpha_{yy}^{\,*}$ are controlled by the flexible directions:

$$\left.\begin{aligned}
\alpha_{xx}^{\,*} &= d_{1x}^{\,2}\alpha_{xx} + d_{1x}d_{1y}\left(\alpha_{xy}+\alpha_{yx}\right) + d_{1y}^{\,2}\alpha_{yy} \\
\alpha_{xy}^{\,*} &= d_{1x}d_{2x}\alpha_{xx} + d_{1y}d_{2x}\alpha_{yx} + d_{1x}d_{2y}\alpha_{xy} + d_{1y}d_{2y}\alpha_{yy} \\
\alpha_{yx}^{\,*} &= d_{1x}d_{2x}\alpha_{xx} + d_{1x}d_{2y}\alpha_{yx} + d_{1y}d_{2x}\alpha_{xy} + d_{1y}d_{2y}\alpha_{yy} \\
\alpha_{yy}^{\,*} &= d_{2x}^{\,2}\alpha_{xx} + d_{2x}d_{2y}\left(\alpha_{xy}+\alpha_{yx}\right) + d_{2y}^{\,2}\alpha_{yy}
\end{aligned}\right\} \tag{25}$$

In Eq. (25), $d_{1x} = \cos\theta_1$, $d_{1y} = \sin\theta_1$, $d_{2x} = \cos\theta_2$ and $d_{2y} = \sin\theta_2$. Inserting directional cutting coefficients, Eq. (25), into Eq. (24), eigenvalues become:

$$\left.\begin{aligned}
&\lambda^* = \frac{-a_1 \pm \sqrt{a_1^{\,2} - 4a_0}}{2a_0} \\
&\textit{here, } a_1 = \left(\cos^2\theta_1 + \cos^2\theta_2\right)\alpha_{xx} \\
&\qquad + \left(\cos\theta_1\sin\theta_1 + \cos\theta_2\sin\theta_2\right)\left(\alpha_{xy}+\alpha_{yx}\right) \\
&\qquad + \left(\sin^2\theta_1 + \sin^2\theta_2\right)\alpha_{yy} \\
&\textit{and} \\
&a_0 = \left(\alpha_{xx}\alpha_{yy} - \alpha_{xy}\alpha_{yx}\right)\left(\cos\theta_1\sin\theta_1 - \cos\theta_2\sin\theta_2\right)^2
\end{aligned}\right\} \tag{26}$$

where α_{xx}, α_{xy}, α_{yx} and α_{yy} are defined in Eq. (4).

Due to non-orthogonal flexible directions, from Eq. (26), it is observed that the eigenvalues are not only function of K_r and radial immersion, but also feed direction. Therefore, when the modes are not orthogonal, chatter stability can be controlled by changing the feed direction.

The relative chatter stability index (CSI) analysis can be conducted following the formulations in the previous section (Eqs. (9)–(19)) and the final relative asymptotic stability index can be postulated as:

$$CSI = \frac{\lambda^*}{a} \tag{27}$$

where λ^* is computed from Eq. (24).

4. Verification of 2D asymptotic CSI

This section focuses on the verification of the proposed asymptotic chatter stability index for 2D orthogonal and non-orthogonal cases and they are compared against the Budak and Altintas' analytical solution from [2].

Parameters for the 2D orthogonal case, $\Phi_{xx}(i\omega) = \Phi_{yy}(i\omega)$, are given in Table 2. The contour plot of the analytically solved asymptotic stability limit is shown in Fig. 15 (a) and the contour plot of the proposed geometry based asymptotic stability index is shown in Fig. 15 (b). Note that, in order to ensure linear vibration, the immersion is kept below 54[deg] for Kr = 0.6 (See Eq. (7)). From Fig. 15, it can be seen that the proposed geometry-based stability index is simply a scaled version of analytical stability solution from [2]. As the immersion is increased the asymptotic depth of cut decreases gradually and the feed direction does not have any effect on the stability.

Next, the non-orthogonal case is studied. In this case, one of the flexible directions is aligned with the X axis and the other one is rotated 30 [deg] from the X axis. The dynamics are kept identical as given in Table 2. Contour plot of the analytical asymptotic stability limit and the CSI index are compared in Fig. 16. In Fig. 16 (b), the white (blanked) region indicates that vibration is exhibiting an elliptical trajectory and proposed CSI does is not capable of predicting the relative stability. Nevertheless, in linear vibration region, the proposed CSI index can predict relative stability accurately. As observed, chatter stability can be increased by manipulating the feed direction and radial immersion. This is similar to the result obtained from Section 2. For instance, Fig. 16 can be used to select set of immersion and feed directions jointly to maximize the MRR without the need for changing spindle speed. Because the approach is geometry-based, it can be implemented efficiently in CAD/CAM systems for process planning.

Table 2. Process and dynamics coefficients

$m_x = m_y$	Mass [kg]	11
$c_x = c_y$	Damping coefficient [N(m/s)]	300
$k_x = k_y$	Spring coefficient [N/m]	10e6
K_t	Tangential cutting coefficient [MPa]	100
K_r	Ratio between radial and tangential cutting coefficient	0.6

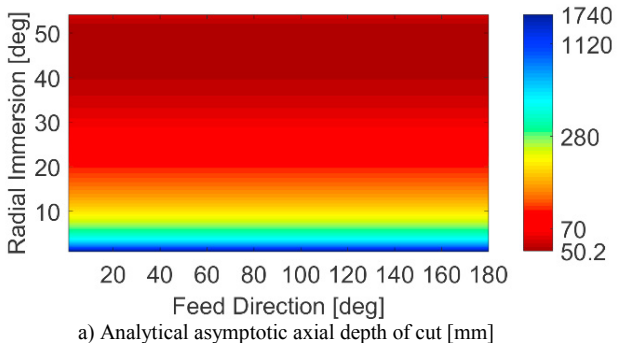

a) Analytical asymptotic axial depth of cut [mm]

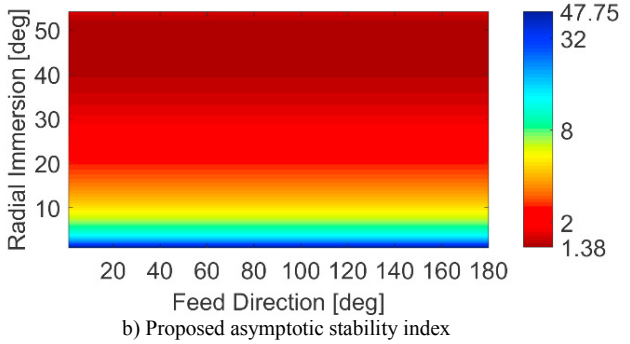

b) Proposed asymptotic stability index

Fig. 15. Analytical and proposed asymptotic stability limit

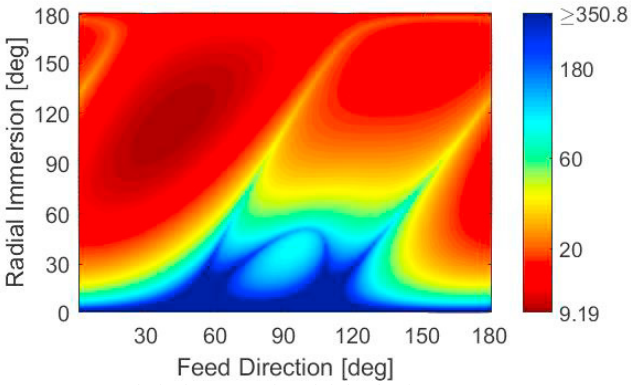

a) Analytical asymptotic axial depth of cut [mm]

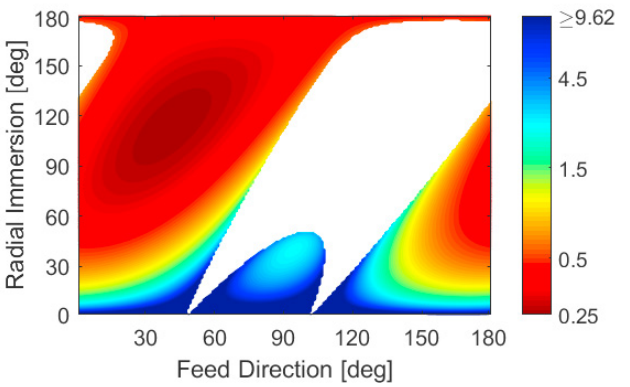

b) Proposed asymptotic stability index

Fig. 16. Analytical and proposed asymptotic stability limits

5. Conclusion

Overall, this paper analyzed effect of directional relationships on chatter stability in peripheral milling. The tool feed direction is considered to be an optimization parameter for maximizing the stability of the milling process. Based on set of directional relationships, a geometry based asymptotic chatter stability index (CSI) is proposed to improve chatter stability. Note that, asymptotic stability limit controls relative chatter stability and hence it does not depend on spindle speed. It is easier to compute and implement in process planning.

Three cases are analyzed where the structure is flexible only in one direction, flexible in two orthogonal directions and in two non-orthogonal directions. When there is only a single dominant flexible direction, it is possible to optimize the feed direction to attain significantly higher MRR. In theory, unlimited chatter free MRR can be attained. However, when the structure exhibits orthogonal modes, regeneration cannot be controlled by changing feed direction. Finally, if the modes are not orthogonal, both feed direction and radial immersion needs to be utilized to optimize the MRR.

Acknowledgment

This research is supported by NSF's Academic Liaison with Industry (GOALI) Award Number: 1661926.

References

[1] Y. Altintas, M. Weck, 2004, Chatter Stability of Metal Cutting and Grinding. Annals of CIRP, Vol. 53/2, pp. 619-642

[2] Y. Altintas and E. Budak, 1995, Analytical prediction of stability lobes in milling. Annals of CIRP, Vol. 44/1, pp. 357-362

[3] M. Weck, Y. Altintas, C. Beer, 1994, CAD Assisted Chatter-Free NC Tool Path Generation in Milling. International Journal of Machine Tools and Manufacture, Vol. 34/6, pp. 879-891

[4] E. Shamoto and K. Akazawa, 2009, Analytical Prediction of Chatter Stability in Ball End Milling with Tool Inclination. Annals of CIRP, Vol. 58/1, pp. 351-354

[5] E. Shamoto, S. Fujimaki, B. Sencer, N. Suzuki, T. Kato, R. Hino, 2012, A novel tool path/posture optimization concept to avoid chatter vibration in machining - Proposed concept and its verification in turning. Annals of CIRP Annals – Manufacturing Technology, Vol.61/1, pp. 331-334.

[6] L. T. Tunc, D. Stoddart, 2017, Tool path pattern and feed direction selection in robotic milling for increased chatter-free material removal rate. The International Journal of Advanced Manufacturing Technology, Vol. 89/9-12, pp. 2907-2918

[7] Z. Pan, H. Zhang, Z. Zhu, J. Wang, 2006, Chatter analysis of robotic machining process. Vol. 173, pp. 301-309

[8] F. Koenigsberger and J. Tlusty, 1967, Machine Tool Structures-Vol. I: Stability Against Chatter. Permagon Press

[9] S. A. Tobias, 1965, Machine Tool Vibration. Blackie and Sons Ltd

[10] H. E. Merrit, 1965, Theory of Self Excited Machine Tool Chatter. Journal of Engineering for Industry ASME, Vol. 17, pp. 447-454

[11] S. G. Chen, A. G. Ulsoy, Y. Koren, 1997, Computational Stability Analysis of Chatter in Turning. Journal of Manufacturing Science and Engineering, Vol. 119/4, pp. 457-460

[12] Y. Altintas, 2000, Manufacturing Automation: Metal Cutting Mechanics, Machine Tool Vibrations, and CNC Design. 1st ed., Ed. Cambridge University Press, NY, USA

[13] M. Weck, 1984, Handbook of Machine Tools, Metrological Analysis and Performance Tests, John Wiley and Sons, 4

[14] V. Thevenot, L. Arnaud, G. Dessein, G. Gazenave-Larronche, 2006, Influence of Material Removal on the Dynamic Behaviour of Thin-walled Structures in Peripheral Milling. Machining Science and Technology, Vol. 10/3, pp. 275-287

[15] E. Budak, Y. Altintas, 1995, Modeling & Avoidance of Static Form Errors in Peripheral Milling of Plates. International Journal of Machine Tools & Manufacture, Vol. 35/3, pp. 459-476

[16] Y. Altintas, M. Eynian, H. Onozuka, 2008, Identification of Dynamic Cutting Force Coefficients & Chatter Stability with Process Damping. Annals of CIRP, Vol. 57, pp. 271-274

[17] R. Sridhar, R. E. Hohn, G. W. Long, 1968, A Stability Algorithm for the General Milling Process. Journal of Engineering for Industry, Vol. 90/2, pp. 330-334

[18] Y. Chen, F. Dong, 2013, Robot machining: recent development and future research issues. International Journal of Advanced Manufacturing Technology, Vol. 66, pp. 1489-1497

[19] E. Abele, J. Bauer, M. Pischan, O. Stryk, M. Friedmann, T. Hemker, 2010, Prediction of the Tool Displacement for Robot Milling Applications Using Coupled Models of an Industrial Robot And Removal Simulation. 2nd International Conference Process Machine Interactions, Vancouver, Canada

[20] Z. Pan, H. Zhang, 2008, Robotic machining from programming to process control: a complete solution by force control. Industrial Robot, Vol. 35/5, pp. 400-409

[21] S. Mejri, V. Gagnol, T. P. Le, L. Sabourin, P. Ray, P. Paultre, 2016, Dynamic characterization of machining robot and stability analysis. The International Journal of Advanced Manufacturing Technology, Vol. 82, pp. 351-359

[22] J. J. Wang, C. F. Sung, 2017, Trajectories of forces and displacements in stable and unstable milling. The International Journal of Advanced Manufacturing Technology, Vol. 89/9-12, pp. 2803-2819

[23] A. Gasparetto, 1998, A System Theory Approach to Mode Coupling Chatter in Machining. Journal of Dynamic Systems, Measurement, and Control, Vol. 120/4, pp. 545-547

[24] B. Stone, 2014, Extension of Chatter Theory. Chatter and Machine Tools, pp. 27-55